Industrial Crops & Products 207 (2024) 117729

Contents lists available at ScienceDirect

Industrial Crops & Products

journal homepage: www.elsevier.com/locate/indcrop

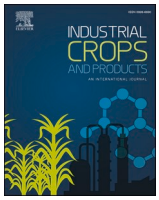

Achieving ultra-tear resistant high-performance natural rubber nanocomposite via bio-inspired lignocellulosic compatibilization

Alireza Hosseinmardi [a], Nasim Amiralian [a], Darren J. Martin [b], Pratheep K. Annamalai [a,c,d,e,*]

[a] Australian Institute for Bioengineering and Nanotechnology (AIBN), The University of Queensland, Brisbane 4072, QLD, Australia
[b] School of Chemical Engineering, The University of Queensland, Brisbane 4072, QLD, Australia
[c] School of Agriculture and Food Sustainability (AgFS), The University of Queensland, Brisbane 4072, QLD, Australia
[d] Centre of Future Materials (CFM), University of Southern Queensland, Toowoomba 4350, QLD, Australia
[e] School of Agriculture and Environmental Sciences (SoAES) University of Southern Queensland, Toowoomba 4350, QLD, Australia

ARTICLE INFO

Keywords:
Cellulose nanofibre
Lignin
Nanocomposites
Natural rubber latex
Elastomer
Tear resistance
Toughness

ABSTRACT

Elastomers which are strong, tough, and resistant to tearing, are highly attractive for engineering applications such as conveyer belts, high-performance seals, tires, and soft robotics. Enhancing these properties for natural rubber materials is possible by utilizing nanoscale fillers, however the nanocomposite approach remains challenging because (a) nanofillers can impede latex molecular crosslinking, and (b) reduce the material's inherent elasticity and compliance. This study demonstrates an approach to prepare ultra-strong, tear-resistant natural rubber nanocomposites using cellulose nanofibers decorated with nanoscale lignin. The reinforcement of latex with 0.1 wt% cellulose nanofibre compatibilized with 0.5 wt% lignin resulted in a 256% improvement in tear strength, 95% in tensile strength, and 50% in toughness, while retaining the elongation at break. Such a simultaneous improvement in tensile and tear properties has not been previously achieved through the latex casting method with any other fillers, and herein it is attributed to the nanoscale reinforcement efficiency of nanofibre coupled with enhanced interfacial adhesion between nanofibers and NR latex with the introduction of nanoscale lignin. This compatibilization approach has also resulted in improved resilience in the nanocomposites, as evidenced by the cycling loading and unloading analysis.

1. Introduction

Elastomers that exhibit high extensibility without stiffening, strength, and reversibility even after several cycles of deformation are highly attractive for a wide range of industrial applications, from gloves and soft robots to seals and tires (Ducrot et al., 2014; Millereau et al., 2018; Zeng et al., 2018). The strength and toughness of elastomers can be chemically enhanced by increasing the cross-linking density and tuning the polymer chain length between the crosslink points, introducing multimodal molecular weight distribution, heterogeneity in the network, and viscoelasticity through copolymerization (Ducrot et al., 2014; Ducrot et al., 2015; Millereau et al., 2018). Strategies for toughening new polymer architectures with networks formed through hydrogen and coordinative bonds are also pursued (Galant et al., 2020). The physical methods that promote strain-induced crystallization (strain-hardening), energy dissipation, and crack resistance, such as pre-stretching, incorporation of micro- to nano-scale fillers, and reactive compatibilization are also explored (Ducrot et al., 2014; Dwivedi et al., 2020; Hosseinmardi et al., 2017; Lay et al., 2020). The physical methods are cost-effective, scalable, and often adaptable to classical polymer processing techniques. The best property profile can be essentially achieved by combining chemical crosslinking and physical reinforcement methods.

Natural rubber (NR) latex is commonly used in manufacturing elastomeric engineering products. The promotion of a homogeneous network formation throughout the NR matrix by classical vulcanization chemistry remains an ongoing challenge (Ducrot and Creton, 2016; Ikeda et al., 2009), as an increase in crosslink density of NR matrix above a certain limit fails to improve the crack resistance due to the brittle failure mechanism that ensues upon uniaxial deformation. To circumvent this challenge (or to retain its intrinsic hyper-elastic properties while improving strain stiffening) the incorporation of nanoscale fillers into NR has been intensively explored in the last decade. In comparison to microscale fillers, nanofillers offer a higher interfacial surface area

* Corresponding author at: Australian Institute for Bioengineering and Nanotechnology (AIBN), The University of Queensland, Brisbane 4072, QLD, Australia.
E-mail addresses: p.annamalai@uq.edu.au, pratheep.annamalai@usq.edu.au (P.K. Annamalai).

https://doi.org/10.1016/j.indcrop.2023.117729
Received 9 August 2023; Received in revised form 25 October 2023; Accepted 26 October 2023
Available online 8 November 2023

and promote energy dissipation, and strain-induced crystallization upon uniaxial deformation (Ozbas et al., 2012; Toki et al., 2013; Xue et al., 2019).

Global concerns about the future of the earth, including sustainability and occupational health awareness, have led to countless efforts to substitute petroleum-based raw materials and inorganic nanomaterials with those derived from green, eco-friendly, renewable, and sustainable resources (Chen et al., 2022; Jiang et al., 2018). So, biobased nanomaterials have gained tremendous attention as an alternative source in many industrial applications including the processing of high-performance nanocomposites (Abid et al., 2021; Chang et al., 2021). Also, with increasing reasonable concerns about the accumulation of bio-waste from pulping industries and as byproducts from food and agricultural industries, it is a timely effort to transform biomass wastes into value-added chemicals and sustainable nanomaterials for advanced materials applications (Basti et al., 2022; Gil, 2021; Guimarães et al., 2022; John et al., 2022). Therefore, the approach of incorporating environmentally sustainable and safe bio-based nanomaterials such as lignocellulosic nanofillers represents the most attractive way forward, as these nanomaterials offer additional attributes of renewability, biodegradability, biocompatibility, and less toxicity (Aziz et al., 2022; Jagadeesh et al., 2021; Sepahvand et al., 2023; Zhang et al., 2022).

Advances in the processing of lignocellulosic-based nanomaterials with various morphologies from different bio-based sources and desired surface chemistries have made nanocellulose as a versatile candidate to be incorporated into different products such as NR nanocomposites (Chang et al., 2021; Kazemi et al., 2022b; Roy et al., 2021). Also, about 700 million years of evolution of the plant's lignocellulosic biomass native structure effectively compatibilizers the hydrophilic polysaccharide components, lignin-like aromatic compounds and paraffinic oils. This perspective indeed offers some inspiration for addressing challenges in interfacial compatibility in rubber nanocomposites with hydrophilic fillers.

As the main component of the lignocellulosic biomass, nanocellulose can be isolated in the shape of rod-like cellulose nanocrystal (CNC), filament-like or web-like cellulose nanofiber (CNF) through various combinations of chemical, enzymatic and mechanical treatments, and incorporated into NR materials improving stiffness, strength, toughness and wear resistance (Gao et al., 2021; Kazemi et al., 2022a; Sirviö et al., 2020). However, the presence of hydroxylic groups on cellulose makes it extremely hydrophilic, moisture absorbent, and strongly self-associating with other cellulose through hydrogen bonding. This makes it very difficult to disperse homogeneously and efficiently in NR as a hydrophobic matrix (Chang et al., 2021; Olonisakin et al., 2022; Roy et al., 2021; Yasin et al., 2021). The incorporation of such hydrophilic fillers in NR latex through the industrially relevant process (latex dipping and casting) achieving broader material property profiles (i.e. improving tensile and tear properties without compromising on inherent soft elastomeric properties) still remains very challenging.

In our previous studies, we have demonstrated that residual lignin in CNF has been beneficial for improving interfacial compatibilization between the CNF and NR matrix to improve overall tensile properties upon uniaxial elongation (Hosseinmardi et al., 2017). Notably, this residual lignin composition can be readily tuned to tailor the surface energy of the CNF for a wide range of polymer matric (Hosseinmardi et al., 2018). Also, from a processing perspective, the dispersion of lignin in NR latex was observed to enhance the colloidal stability of latex and improve the physical properties of rubber films (Hosseinmardi et al., 2021).

Building upon these foundational findings, this study aims to further advance the nanocomposite preparation approach by combining i) the reinforcement effect of CNF, with the added benefits of lignin to enhance colloidal stability/dispersibility of natural rubber latex. Moreover, it is hypothesized that incorporation of lignin will be compatible with CNF surface and enhance the dispersibility of CNF in the host matrix. Hence, the innovative compatibilization approach (Fig. 1) involves the modification (coating) of the nanofibers with lignin, which is inspired from the natural lignin carbohydrate complex formation in growing lignocellulosic plant biomass. By demonstrating the process to improve properties through a bio-inspired compatibilisation, and discussing the structural aspects, hysteresis behavior and swelling characteristics, this study introduces an advanced methodology for NR nanocomposites with lignocellulosic nanomaterials.

2. Materials and methods

Commercially centrifuged natural rubber latex (Lalan Rubbers Pvt Ltd) was used for compounding with nanofillers. The nanofillers were included cellulose nanofibers was derived from spinifex (*T. pungens)* grass (generously supplied by Bulugudu limited) after washing in hot water for three times, drying, grinding to powder, alkali treatment (with 2% w/v aq. solution of NaOH for 2 h at 80 °C, followed by washing several times by filtration and then nanofibrillation through high pressure homogenization (HPH) as described previously (Hosseinmardi et al., 2018), commercial OSL, and vulcanizing agents (detailed in the supporting information. The compounded natural rubber (NR) latex was stirred by using an overhead stirrer at 150 rpm for 30 min. The vulcanizing agents (supplied from Tiarco Chemical (M) Sdn Bhd) and nanofillers are listed in Table S1. High ammonia content commercialized centrifuged latex was supplied from Lalan Rubbers Pvt Ltd and used as a compounded natural rubber (CNR) latex. The product contained 60% NR (cis 1,4 polyisoprene, $(C_5H_8)_n$), obtained by wounding and sapping the rubber tree (*Hevea brasiliensis*). The ammonia content and pH value were 0.55% and 10.5, respectively.

The control NR and the nanocomposites with OSL, CNF, and OSL-CNF dispersed were prepared following the protocol summarized in Fig. 2 at the second step dilution of NR. The ultimate solids content and pH mixture were adjusted to 47% and 10.5, respectively. Then, the prepared mixture rested at room temperature for an extra 24 h (maturation period) before casting into the flat glass molds. Cast films were kept at room temperature overnight to become dry films. The dried films were pre-cured for 20 min in a convection oven at 100 °C. The obtained films were dusted with microscale calcium carbonate powder (to prevent film tackiness) and leached with hot DI water (65 °C) for 15 min. Finally, films were cured at 100 °C for 1 h in a convection oven. All prepared samples were rested for at least 48 h within laboratory conditions (room temperature and 50% humidity) before further characterization. Samples were labelled according to the loading weight of CNF and OSL. For example, 0.1 wt% CNF-2 wt% OSL/NR consists of 0.1 wt% CNF and 2 wt% OSL.

Further details on characterisation methods and conditions for nanoscale lignin dispersions, CNF modification and nanocomposite samples are described in supporting information.

3. Results and discussion

As inspired from natural interactions of the main components of plant resources, lignin and cellulose at nanoscale in native lignocellulosic biomass, the CNF was modified with OSL after dissolution (Nishimura et al., 2018). Firstly, the OSL was dispersed in alkaline aqueous media and then the CNF was mixed to form OSL modified CNF. This mixture was incorporated into NR latex media for nanocomposite preparation through casting process including industrially relevant leaching steps. The morphological differences of CNF derived from spinifex grass biomass and those modified (coated) with OSL were investigated using transmission electron microscopy (TEM). Fig. 3a-c represents a high aspect ratio CNF with an average width of 28 nm and length of over 10 μm. When the CNF was modified with an aqueous solution of OSL (prepared by increasing pH), the CNF was decorated with nanoscale OSL causing a nominal increase in the thickness of the nanofiber. For example, the average width of CNF increased to 40 nm

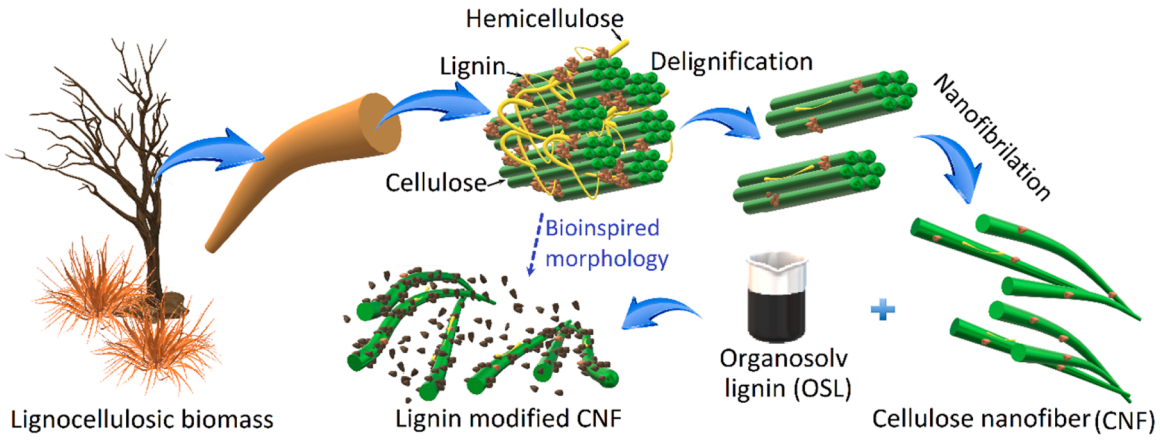

Fig. 1. Bio-inspired modification of cellulose nanofiber with organosolv lignin for improving the dispersibility and compatibilization.

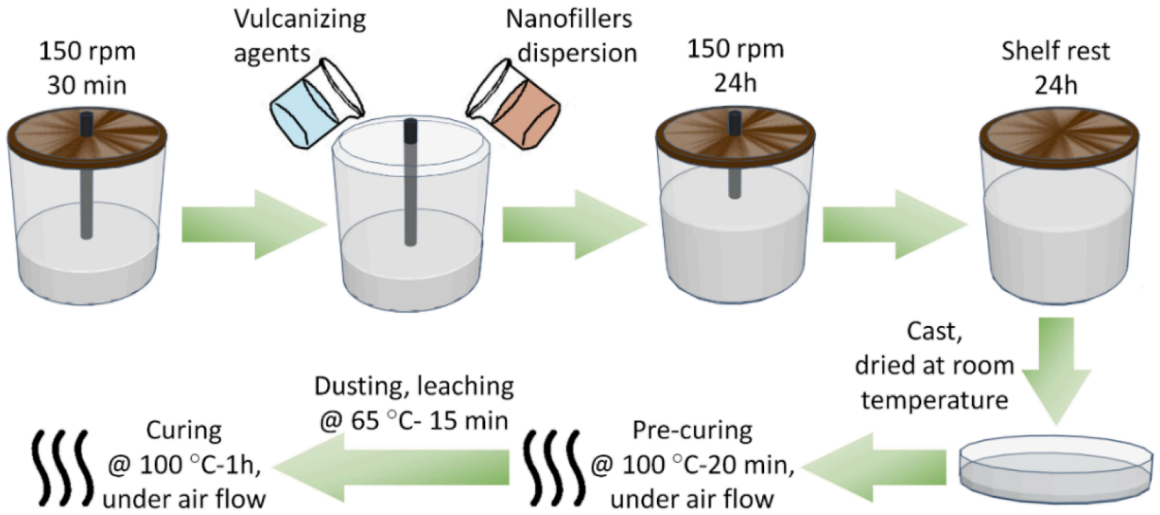

Fig. 2. The schematic diagram for preparation methodology of control, OSL/NR, CNF/NR, and CNF-OSL/NR nanocomposites.

and 42 nm with 1 and 2 wt% of OSL (Fig. 3d-i), respectively. This can be attributed to either re-agglomeration of CNF in presence of OSL and/or the adsorption of OSL on the surface of CNF. It should be noted that not all OSL coated to the CNF, but they also dispersed well in the aqueous alkaline media which facilitates dispersion of CNF. Such interactions are facilitated by the functional groups (such as phenolic hydroxyls and carboxylic groups) available on both OSL and CNF (Corletto et al., 2022; Hosseinmardi et al., 2021). To study the impact of bio-inspired lignin modified CNF, uncoated CNF and nanoscale lignin on the performance of NR nanocomposite, they were mixed individually at different concentrations with natural rubber latex and other curing agents for further post-vulcanization. The NR nanocomposite films were prepared by casting, drying, dusting with calcium carbonate powder, leaching in hot deionized water and thermal curing.

Fig. 4 shows the tensile properties of control NR and nanocomposite samples with CNF, OSL and OSL modified CNF. The dispersion of OSL alone at 0.5 wt% and 1 wt% into the NR matrix increased the tensile strength of NR by 13%, and 29%, respectively. This was simultaneously accompanied by an improvement in tensile strain. For instance, the tensile strain of the control sample increased from 1778% to 1921% for 0.5 wt% OSL/NR, and to 1937% for 1 wt% OSL/NR. This could be attributed to the enhanced dispersion of OSL throughout the NR matrix, resulting in good interactions between the latex and OSL and protection against any possible thermo-oxidative degradation during curing at high temperatures (Barana et al., 2016; Bokobza, 2004). A further increase in loading level to 2 wt% has resulted in a slight decrease in tensile strength and elongation at break. This can be attributed to the heterogeneous dispersion of OSL due to agglomeration at the higher loading. Thus, heterogeneous dispersion of the filler in the NR matrix results in inadequate OSL/NR adhesion (i.e. filler-filler interaction over filler-matrix interactions) and affects the ultimate mechanical performance during tensile deformation of the NR nanocomposite sample (Setua et al., 2000; Tan et al., 2015). This trend of improvement in tensile properties with OSL in post-vulcanized NR latex systems is consistent with the improvements observed with pre-vulcanized NR system, confirming the compatibility OSL with NR matrix (Hosseinmardi et al., 2021).

The incorporation of 0.1 wt% of CNF in NR caused a significant increase in the tensile stress and tensile strain of nanocomposites, compared to the control. The tensile strength and elongation at a break of 0.1 wt% CNF/NR resulted in a 22 MPa (56% improvement) and 1999% (12% improvement), respectively. These improvements are concurrent with our previous observations of pre-vulcanized NR latex/spinifex CNF nanocomposites prepared through the casting method (Hosseinmardi et al., 2018; Hosseinmardi et al., 2017). The improvements are attributed to the enhanced dispersion of nanofibers throughout the matrix and filling of the interstitial gaps between the latex particles which efficiently transfer shear stress from the matrix to fillers more efficiently (Annamalai et al., 2014; Hosseinmardi et al., 2017).

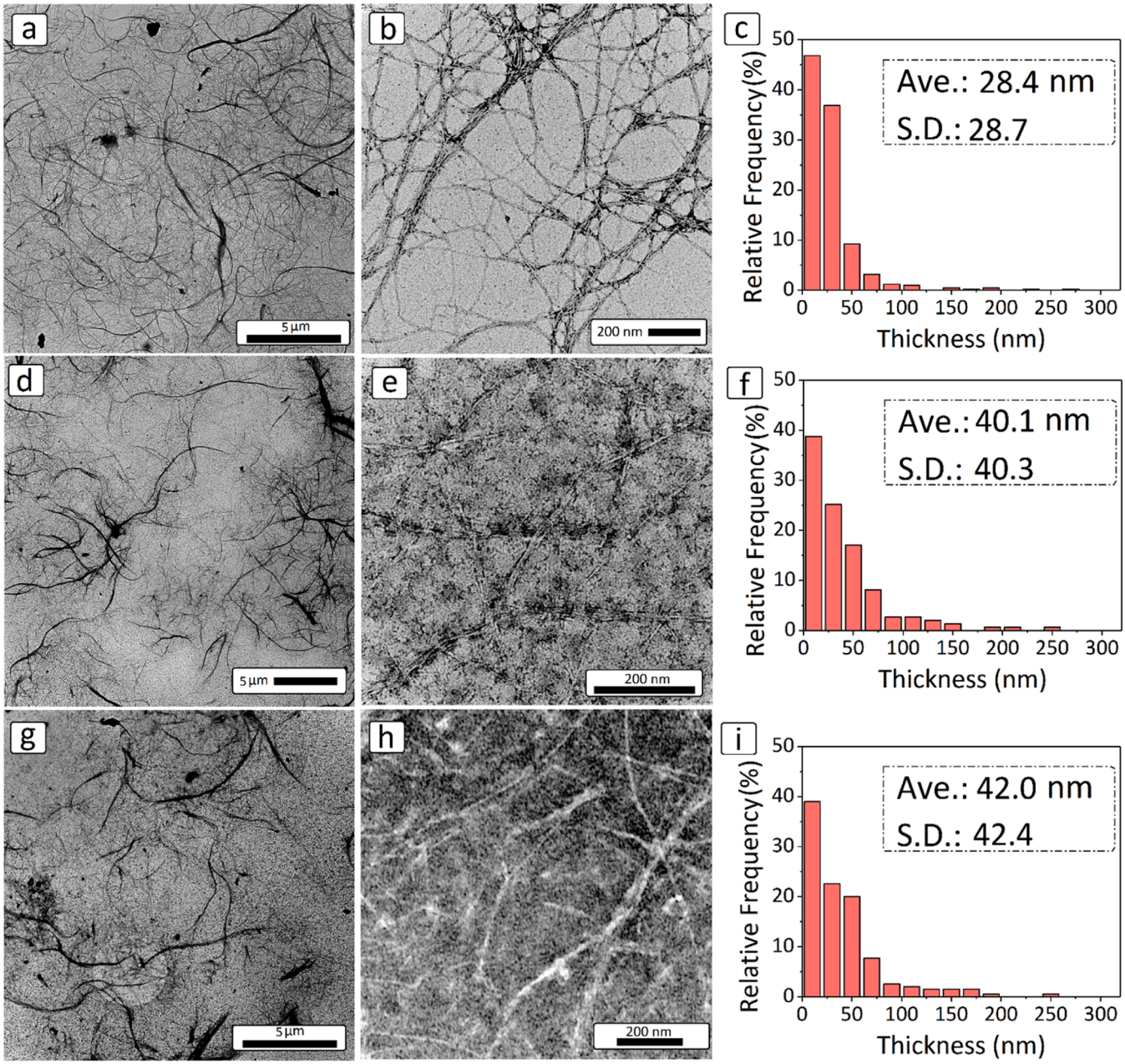

Fig. 3. TEM images and CNF thickness distribution of (a-c) CNF, (d-f) 1 wt% OSL-CNF and (g-i) 2 wt% OSL-CNF samples at different magnifications.

The incorporation of 0.1 wt% CNF with 0.5 wt% of OSL remarkably improved mechanical properties Fig. 4. The tensile strength and elongation at break were improved over 95% (28 MPa) and 17% (2079%), respectively compared to control NR. This improvement is significantly higher than that observed with 0.1 wt% CNF or 0.5 wt% OSL alone in the NR matrix. The enhancement of mechanical properties, in addition to providing the hydrodynamic reinforcement effect and the tandem mechanism of protection, is related to OSL's role as a compatibilising agent between CNF and NR (Song and Zheng, 2016). Hence, the modification of CNF with OSL as shown in Fig. 3, facilitated dispersion of CNF in the NR matrix, resulting in enhanced adhesion between CNF and NR that considerably promoted strong filler-polymer interactions and improved strain-hardening effect.

Further increases in loading levels of OSL (1 and 2 wt%) in the CNF-OSL/NR nanocomposites did not exhibit such remarkable improvements, but still showed modest improvements (50%) as compared to the control NR films and comparable improvements (31% and 10%) as their OSL/NR nanocomposite counterparts. This suggests that 0.5 wt% of OSL is optimum to enhance the tensile properties of CNF-OSL/NR nanocomposites. At high loading levels of OSL (1 and 2 wt%), the reinforcement effect of 0.1 wt% CNF becomes insignificant, and no synergistic improvements are observed. Above an optimum level, the agglomeration and presence of OSL in the interstitial space between latex particles might reduce the coalition of the latices and retard the crosslinking reactions. This is reflected as a reduction in elongation at break (Fig. 4b). For instance, compared to 0.1 wt% CNF-0.5 wt% OSL/NR nanocomposite, the nanocomposites with high OSL loading (1 or 2 wt%) in combination with 0.1 wt% CNF showed a significant decrease in elongation. The simultaneous improvements in tensile strength and elongation with nanofillers (OSL, CNF and OSL modified CNF) is reflected in tear strength, toughness, and hysteresis behavior as well.

The tear strength values and pictures of tear crack propagation for the control and nanocomposites are illustrated in Fig. 5a and b, respectively. The tear strength of the control sample was 17.5 Nmm^{-1},

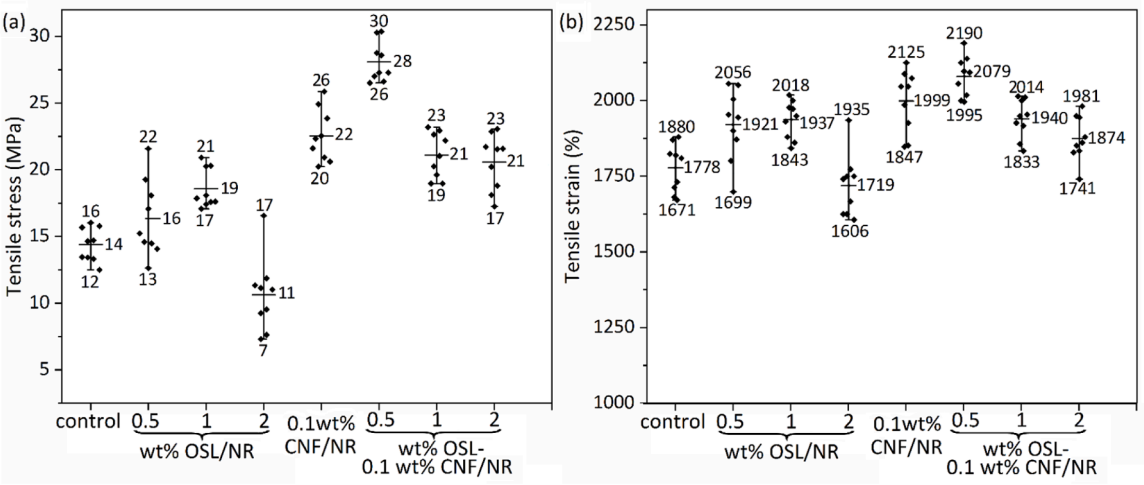

Fig. 4. (a) Tensile stress and (b) tensile strain of control, CNF/NR, OSL/NR and CNF-OSL/NR nanocomposites with different contents of CNF and OSL.

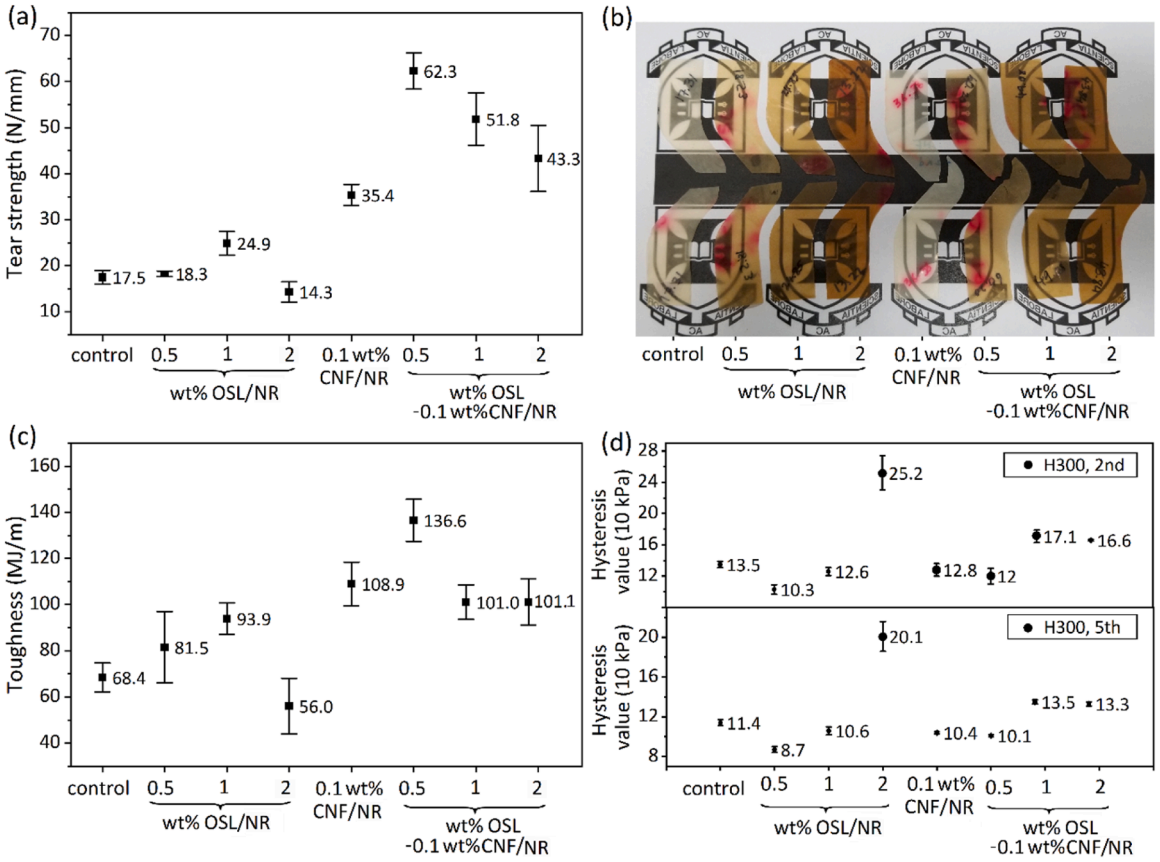

Fig. 5. a) Tear strength, b) pictures of tear crack propagation, c) toughness values and d) hysteresis values of 2nd and 5th cycles at 300% elongation for the control, OSL/NR, CNF/NR and CNF-OSL/NR nanocomposites with different contents of CNF and OSL.

corresponding to a clean break tear. The incorporation of OSL (up to 1 wt%) into the NR matrix caused an increase in the tear strength. For example, the tear strength of 1 wt% OSL/NR increased by 42% compared to the control sample. This is due to the reinforcement effect of dissolved lignin. However, increasing OSL concentration to 2 wt% was observed to decrease the tear strength showing a similar trend in tensile properties. Agglomeration of OSL at higher loadings could be the main reason for the deterioration of tear properties. Although the tear strength of 0.5 and 1 wt% OSL/NR increased, Fig. 5b features clean break tears for these samples, as well as for 2 wt% OSL/NR. These results indicate that cracks propagated easily in one step, involving little energy absorption.

Incorporation of 0.1 wt% CNF into NR had a significant influence on the tear strength of NR nanocomposites. As shown in Fig. 5a, the tear strength of 0.1 wt% CNF/NR improved by 102% compared to the control sample. The extraordinary increase in tear resistance was further observed because of the compatibilization of CNF with OSL in NR matrix. The tear strength of 0.1 wt% CNF-0.5 wt% OSL/NR increased to 62.3 Nmm^{-1}, which was 256% higher than the control. However, higher OSL contents (1 and 2 wt%) in CNF-OSL/NR nanocomposites resulted in

lower tear strength compared with 0.1 wt% CNF-0.5 wt% OSL/NR nanocomposite, but still maintained astounding improvements in tear resistance compared to the control NR sample and OSL/NR counterparts. The tear strength of 0.1 wt% CNF-1 wt% OSL/NR and 0.1 wt% CNF-2 wt% OSL/NR were 51.8 Nmm^{-1} and 43.3 Nmm^{-1}, respectively, corresponding to a 196% and 147% tear strength improvement compared with the control sample. CNF/NR and CNF-OSL/NR nanocomposites in Fig. 5b featured the zigzag tear propagation pattern, revealing a high resistance to crack initiation and growth during the tear test. Therefore, further application of energy was necessary during the tear test to achieve the ultimate failure of the specimen, demonstrating that extensive adhesion and crosslinking had occurred between the OSL-coated CNF and NR polymer chains. Moreover, another factor is the influence of dissolved OSL (in NR matrix) that formed a homogenous dispersion of OSL throughout the NR matrix. A similar trend of improvements was observed for toughness as well. The toughness values of 0.5% OSL/NR, 0.1 wt% CNF/NR and 0.5 wt% OSL-0.1 wt% CNF/NR nanocomposites were improved by 19%, 59%, and 100% respectively, as compared to the control (Fig. 5c). This indicates the improvements in ductility and increase in energy required for failure upon compatibilization of CNF with NR matrix by introducing of OSL. Higher loading of OSL into CNF/NR resulted in decreasing trend in improvements, while still maintaining toughness values well above the samples without CNF.

Cyclic uniaxial loading-unloading tensile tests were performed to investigate the viscoelastic properties and hysteresis behavior of the control and NR nanocomposites. The area of the stress-strain loop is known as the '*hysteresis value (kPa)*' and it represents the energy dissipation or loss throughout the polymer matrix. The hysteresis behavior of the control and NR nanocomposites was monitored from the five continuous uniaxial loading-unloading stress cycles up to a strain of 100%, 300%, and 700% as shown in Fig. S2, where the higher strain range was applied after completion of the 5th cycle. The hysteresis values of the 2nd and 5th cycles at all measured strains are presented in Table S3, while at 300% strains are plotted in Fig. 5d. Overall, the higher hysteresis values for the nanocomposites as compared to the control indicate the increased energy dissipation by the physical/chemical network and/or the reinforcement effect of the incorporated fillers. The hysteresis values for all samples decrease with increasing number of

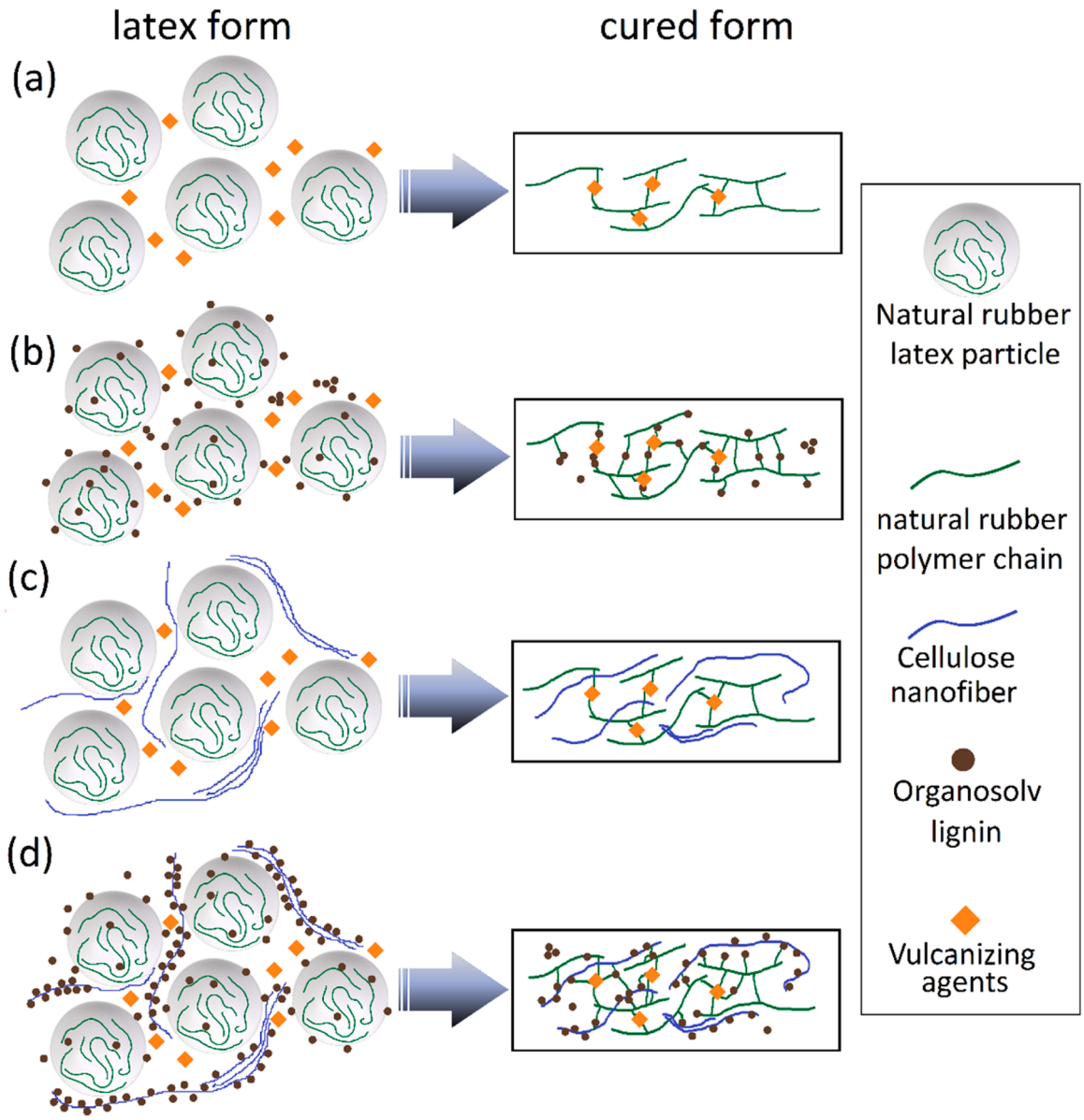

Fig. 6. Schematic representation showing the dispersion of nanofillers in a latex and cured form of compounded natural rubber (a) a control sample, (b) CNF/NR nanocomposites, (c) OSL/NR nanocomposites and (d) CNF-OSL/NR nanocomposites.

loading-unloading cycles, specifically after the first cycle at the same level of strain, which indicates the typical stress-softening behavior of elastomers. This is also referred to *Mullin's effect* which is associated with bond rupture, molecular slippage, filler rupture and disentanglement that occur during the previous cycle of loading and unloading (Bhattacharyya et al., 2008; Diani et al., 2009; Mullins, 1969).

The comparison of hysteresis values of the control and nanocomposite samples after the 2nd cycle (Table S3) at each strain showed a moderately decreasing trend upon the incorporation of nanofillers (OSL, CNF or OSL modified CNF). For instance, the hysteresis values of the control, 0.1 CNF/NR, 1 wt% OSL/NR and 0.1 wt% CNF-1 wt% OSL/NR nanocomposites in the 2nd cycle at 700% were 28.7, 26.6, 26.8 and 28.1 MPa, respectively. This shows that incorporated nanofillers did not have significant stiffening effect. These results contrasted with the hysteresis values of pre-vulcanized NR nanocomposites, which showed a significant increase in hysteresis values after introducing OSL and CNF-OSL into the polymer matrix (Hosseinmardi, 2019). This could be due to the semi-crosslinked nature of pre-vulcanized NR, where nanofillers were limited to embedding in the interstices and boundary regions of the NR latex particles (Fig. 6). However, in the post vulcanizable NR system, nanofillers (CNF, OSL, and CNF-OSL) were proposed to have the "further freedom" to disperse throughout the uncrosslinked NR matrix. This retention and even slight enhancement of resilience is a very important factor for many rubber products and this route to latex nanocomposite preparation, although not fully optimized here and ultimately needing further tech-transfer to a commercial latex facility, looks most preferable from this standpoint.

Furthermore, the difference between the hysteresis values after the 2nd and 5th cycles indicates the irreversible changes in the sample (due to NR chain orientations), where smaller differences are preferred for resilience and energy dissipation. This difference for the control was about 25.9 (10kPa) at 700% strain, whereas for the 0.5 wt% OSL/NR nanocomposite, the value was only 11.7 (10 kPa). Further increases in the OSL loading increased the difference in hysteresis values of the 2nd and 5th cycles to 19.4 (10kPa) and 38.7 (10 kPa) for 1 wt% and 2 wt% OSL/NR nanocomposites. This could be related to enhanced irreversible changes in molecular architectures (during stretching) due to ruptures in secondary bonding such as hydrogen bonding and van der Waals interactions between nanofillers and NR, which could reduce the reorientation of rubber chains.

For 0.1 wt% CNF/NR and 0.1 wt% CNF-0.5 wt% OSL /NR incorporated nanocomposites, this difference was about 16 (10 kPa) and 16.4 (10 kPa), respectively, which are still lower than observed for the control. This implies that incorporation of 0.5 wt% OSL has not induced any significant irreversible changes effect which could affect the ability to dissipate energy. Further increase in OSL loading (1 or 2 wt%) has increased the differences in hysteresis values of the 2nd and 5th cycles. This may correspond to an increase in molecular friction by increased OSL contents, and irreversible changes during stretching of the nanocomposites.

To understand the influence of nanofillers on the plastic deformation during hysteresis cycles, the residual strain values at zero stress were monitored after the 1st and 5th loading-unloading cycles at a strain of 100%, 300%, and 700% (Table S4). The difference between residual strains after the 1st and 5th cycles at the same strain is referred as 'residual strain shift' which indicates the measure of plastic deformation pronounced upon multiple load cycles. While the plastic deformation is least preferred for elastomers, an increase in residual strain values is attributed to the polymer chain reorientation (in control rubber film) and/or displacement and/or agglomeration of nanofillers (for nanocomposites) after employing certain strain elongations. The residual strain for the control was 11%, 23% and 49% after the 5th cycle completion at 100%, 300% and 700% strain respectively, whereas the residual strain shift at 700% strain was 9%. Upon incorporation of OSL, it showed an increasing trend in residual strain shift values, while still maintaining overall residual strain values at 46%, 43%, and 48% below the control. For example, the residual strain shift of 0.5 wt% OSL/NR, 1 wt% OSL/NR, and 2 wt% OSL/NR at 700% strain, were 5%, 7%, and 11%, respectively. This could be attributed to the interaction between OSL (dissolved and agglomerated at higher loading weight) and the NR host matrix, which acted as a more plastic-like interfacial deformation and associative behavior and prevented specimens from returning to their original dimensions (Sarkanen et al., 1981).

The incorporation of 0.1 wt% CNF into NR did not increase the residual strain (46%), or its shift (6%) compared to the control at 700% strain. The compatibilization of 0.1 wt% CNF with 0.5 wt% OSL in NR has further decreased the residual strain to 44% and its shift around 4%. However, an increase in OSL content to 1 wt% with 0.1 wt% CNF has increased the residual strain (after the 5th cycle at 700% strain) to 59%, attributing to the disentanglement of OSL-coated CNF and NR polymer chains. Another likely mechanism to explain these results could be the rupture of hydrogen bonds between the OSL-CNF network and OSL-coated CNF/NR during stretching, regenerating new hydrogen bonds at newly available sites. Further increase in OSL loading to 2 wt% (in 0.1 wt% CNF-2 wt% OSL/NR), caused agglomeration of OSL in the nanocomposites due to OSL-OSL interactions (Hosseinmardi et al., 2021). Because of such heterogeneous dispersion of OSL in NR matrix, the integrity and tensile properties decreased. This has been reflected in lower residual strain (37%) and its shift (6%) compared with the control sample.

To further understand these properties improvement upon incorporation of nanofillers (OSL, CNF and OSL modified CNF) in NR, structural changes are explained schematically in Fig. 6. It shows the morphological changes upon the dispersion of vulcanizing agents (Fig. 6a) and/or nanofillers (Fig. 6b-d) in an uncrosslinked NR matrix in the form of latex and cured films. Unlike in the pre-vulcanized NR systems where the nanofillers are placed in the boundary of the (optimally crosslinked NR) latex particles and coalescence of soft-particles is controlled, nanofillers can be dispersed throughout the matrix in the post-vulcanized NR system where coalescence of soft-particles is thermodynamically favored. In the post-vulcanization compounding method, vulcanizing agents and nanofillers are mixed in the latex. These components can form physical or chemical bonds with each other while mixing in latex form during the maturation period and curing process. Thus, the nanofillers OSL (Fig. 6b) and CNF (Fig. 6c-d) are homogeneously distributed in the host NR matrix. Therefore, it would be expected that further crosslinking would take place in the post-vulcanized NR system between nanofillers and NR polymer chains, which caused significant improvement in the tensile properties. In the nanocomposite system with OSL-modified CNF (Fig. 6d), the decorated OSL on the surface of CNF could bond either with vulcanizing agents or NR polymer chains promoting crosslinking. This could explain the outstanding tensile and tear strength properties for CNF-OSL/NR nanocomposites. These broader property improvements are related to good adhesion of the nanofillers and cohesive interaction with polymer matrix. These structural morphologies were confirmed by investigating the cross-sections of nanocomposite specimens.

Fig. 7 compares the cryo-fractured (cross sectioned) surfaces of the control and NR nanocomposite samples. The control shows a relatively smooth cross section fracture surface. The addition of OSL (left panel in Fig. 7), in NR latex introduced roughness on the cross-section surfaces. At 2 wt% OSL loading it clearly showed OSL agglomeration in interstitial spaces between latex particles which was attributed to the lowest mechanical properties for this sample. Well dispersed OSL in the NR matrix could enable both OSL/OSL and OSL/NR interactions. At higher concentrations OSL/OSL interactions might be strong enough to form agglomeration. When the CNF (0.1 wt%) was dispersed well into the NR matrix, the cross-section appeared with rough, partially coalesced latex particles and good wavy groove features (Hosseinmardi et al., 2017).

As soon as the CNF was incorporated in combination with OSL (0.5, 1 wt%), the samples showed rough surfaces with wavy groove features indicating enhanced dispersion of CNF, vulcanizing agents and

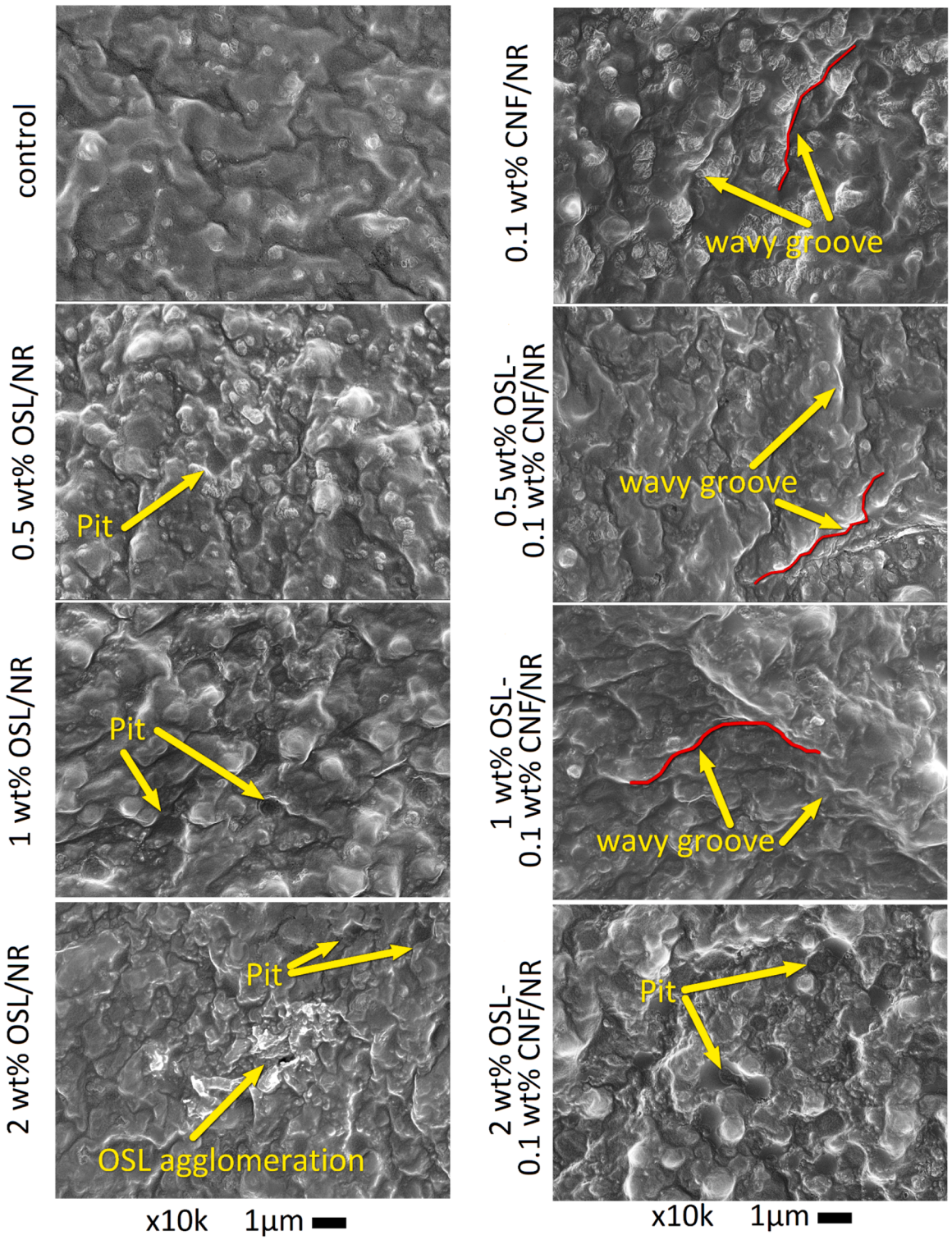

Fig. 7. SEM images of the cryo-fracture surface for control, OSL/NR, CNF/NR and CNF-OSL/NR nanocomposites with different contents of CNF and OSL. The magnification and scale bar are 10 k and 1 μm, respectively.

coalescence of latex particles. This supports enhanced compatibilization and cohesion of OSL modified CNF in NR matrix which was associated with improving the tensile and tear strength properties of the NR nanocomposite samples (Hosseinmardi et al., 2017). In addition, the pit features that were visible on the cryo-fracture surface for 1 wt% OSL/NR did not form in 0.1 wt% CNF-1 wt% OSL/NR. In contrast, the fracture surface morphology of 0.1 wt% CNF-2 wt% OSL/NR differed from 0.1 wt% CNF-(0.5–1 wt% OSL)/NR, with the surface displaying several pits. As discussed earlier, OSL could dissolve in the alkali media and then reprecipitate or coat the surface of CNF to form OSL-coated CNF during drying.

At an optimal loading level (<1 wt%), OSL could act as a compatibilizing agent between CNF and rubber, which enhanced adhesion between nanofillers and polymer chains. Further increase in the OSL concentration promoted OSL/OSL interactions causing agglomeration and congregation around NR latex particles which would decrease the

crosslinking between NR latex particles during the curing process. This also separated them and formed pit features in (1–2 wt%) OSL/NR and 0.1 wt% CNF-2 wt% OSL/NR samples.

Fig. 8a and b illustrate the short term (48 h) and long-term (8 weeks) water uptake properties of the control and nanocomposite samples soaked in DI water. All the samples showed an increasing trend of the water uptake over the period of 8 weeks. Overall, the water absorption can be affected by surface energy and roughness (of film), hydrophilicity of the fillers, adhesion, and compatibility (different interfacial structures) between filler and matrix and crosslinking (Kumar and Singh, 2008; Qiu et al., 2003). The incorporation of OSL in NR reduced the rate of water absorption and the water uptake decreased with increasing OSL content above 1 wt%. This can be attributed to the hydrophobic nature of OSL which can act as cementitious (rigid domain) barrier in the soft matrix. When the 0.1 wt% CNF was incorporated alone, the water uptake rate increased. This is in concordance with our previous observation of the prevulcanized NR system (Hosseinmardi et al., 2017). The water uptake with CNF containing nanocomposites can be attributed to the hydrophilicity of nanofiber which can act as water conduits channeling water molecules further into the host polymer matrix (Annamalai et al., 2014). When the CNF was incorporated in combination with OSL, water uptake was relatively decreased. The lowest (final) water uptake was observed for 2 wt% OSL containing CNF/NR nanocomposite. An increase in the OSL/CNF ratio introduced cementitious rigid phases in the host soft matrix, which decreased the ultimate water uptake. However, it is worth mentioning that increase in OSL content caused agglomeration of OSL affecting cross sectional roughness (as seen in Fig. 7) and hysteresis behavior under cyclic tensile loads.

To understand the effect of CNF and OSL on the swelling ratio, crosslink density and shear modulus of nanocomposites, a swelling test in toluene was employed. Fig. 8c-e shows the swelling ratio, crosslink density and shear modulus of the control and nanocomposites. These results indicated that the swelling ratio of the control sample was affected considerably after introducing nanofillers into the NR matrix. Fig. 8 displays the swelling ratio, or the toluene penetration into the matrix, of all prepared nanocomposites (except 2 wt% OSL/NR) decreased compared to the control sample. This indicated that CNF, OSL and CNF-OSL block suitable solvent uptake voids in NR nanocomposites. Thus, these nanofillers blocked the solvent pathway into the matrix or acted as obstacles to the spread of toluene in the NR matrix (Somaratne et al., 2014). This could be associated with dispersion of these fillers in the matrix, in addition to the effective filler/filler interaction and filler/NR interaction that increased the crosslink density (Fig. 8d). Additionally, the swelling ratio of 2 wt% OSL/NR increased compared to the control sample. This might be attributed to the tendency for OSL to agglomerate at higher loading weights (the swelling ratio of 1 wt% OSL/NR was marginally higher than 0.5 wt% OSL/NR and significantly lower than 2 wt% OSL/NR). Therefore, the interaction of filler/filler (OSL/OSL) was stronger than filler/polymer (OSL/NR polymer chains), which forms voids in the matrix and facilitated toluene penetration into the 2 wt% OSL/NR.

Fig. 8d and e indicated a trend of increasing crosslink density and shear modulus after introducing CNF and OSL into the NR nanocomposites (excluding 2 wt% OSL/NR). These phenomena were consistent with results from mechanical testing, as shown in Fig. 4, Fig. 5 and Table S2. So, it can be concluded that CNF and OSL individually, and in the form of OSL-coated CNF, would enhance the crosslink density via inclusion and interaction (chemically and physically) within the host polymer (NR). According to Somaratne et al., in addition to covalent bond chemical crosslinking between rubber chains and the physical

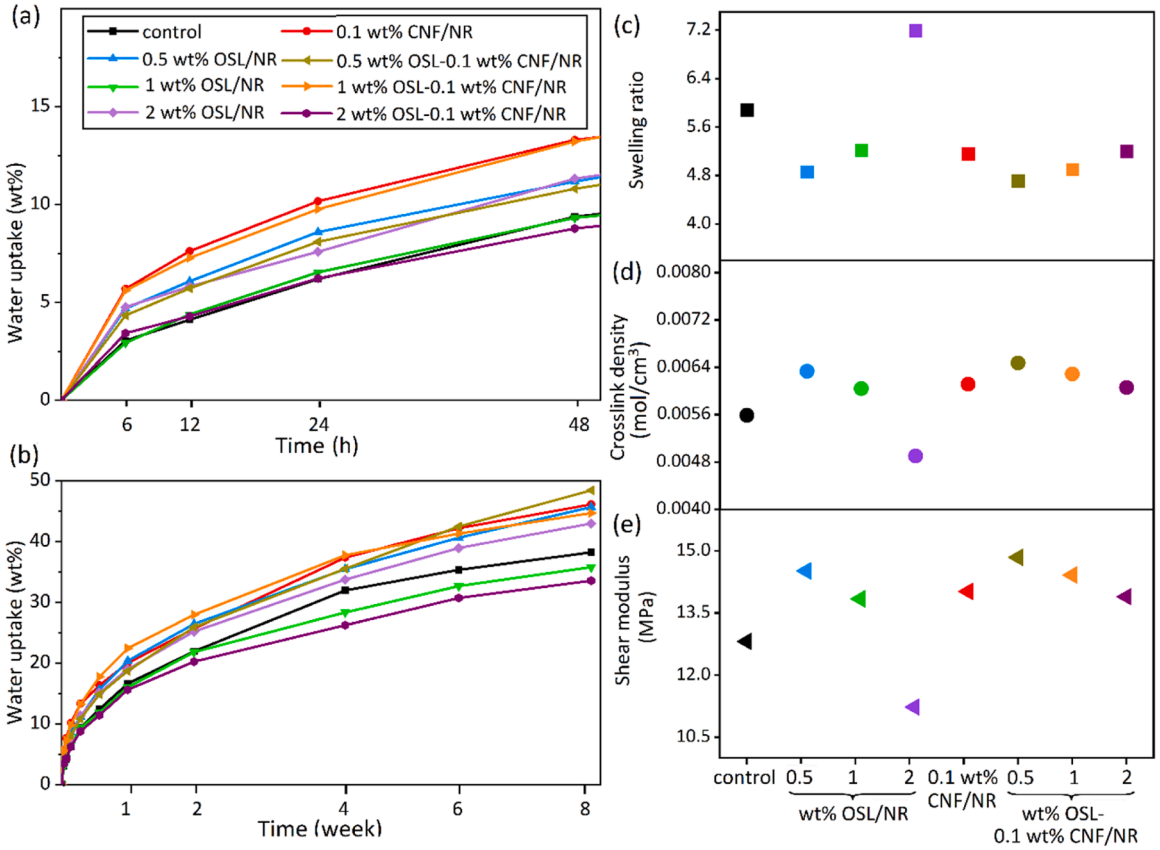

Fig. 8. Solvent absorption properties of the control, CNF/NR, OSL/NR and CNF-OSL/NR nanocomposites with different contents of CNF and OSL, cured at 100 °C for 1 h. (a, b) water uptake for short-term and long-term, c) Swelling ratio, (d) crosslink density and (e) shear modulus determined from swelling of samples in toluene for 5 days.

interaction among fillers, secondary valence bonds occurred between free ends rubber chains and fillers, which corresponded to further enhancement of the crosslink density in NR nanocomposites (Fu et al., 2008; Somaratne et al., 2014). For instance, the highest crosslink density was obtained for 0.1 wt% CNF-0.5 wt% OSL/NR, which exhibited the best tensile properties and tear strength. On the other hand, the lowest tensile properties, tear strength and modulus at 300% and 700% were achieved by 2 wt% OSL/NR, which was due to the smaller crosslink density for this sample.

Also, the effect of OSL and CNF on the thermal stability of NR was studied using thermal gravimetric analysis (TGA, Fig. S1). The attained curves indicated that the onset decomposition temperature (T_{onset}) increased when introducing OSL into the NR latex. This could be attributed to the lower decomposition temperature of OSL compared with the control (Yang et al., 2007). Fig. S1b shows that all samples have thermally decomposed in one-step, and the maximal weight loss temperature (T_{max}) is around 355 °C.

4. Conclusions

In this study, we demonstrated an advanced processing approach for nanocellulose reinforced natural rubber nanocomposites through bio-inspired compatibilisation using lignin. The incorporation of spinifex-derived CNF modified with OSL has afforded a greater improvement property profile as compared to control NR or the nanocomposites with cellulose nanofiber or lignin separately. For example, 0.1 wt% CNF and 0.5 wt% OSL can improve tear strength by 256% and tensile strength by 95%, and toughness by 50% while improving resilience. This is attributed to enhanced compatibilization of CNF with NR in presence of lignin. The cross-sectional analysis using electron microscopy and solvent swelling measurements have supported enhanced adhesion of nanofiber and the NR host matrix in presence of lignin. With these findings, it can be concluded that a bio-inspired compatibilization approach presents a promising strategy for developing ultra-tear-resistant and strong natural rubber nanocomposites. Also, the well-compatibilized nanocomposite materials have significant implications in industrial and engineering fields, particularly for the production of durable tires, conveyor belts, and seals that endure high levels of cyclic mechanical stress and wear. Moreover, these nanocomposites as thin film protective materials hold promise in medical applications, such as the manufacturing of resilient condoms and surgical gloves.

CRediT authorship contribution statement

Alireza Hosseinmardi: Conceptualization, Methodology, Investigation, Validation, Writing – original draft. **Nasim Amiralian:** Supervision, Investigation, Writing – review & editing. **Darren J Martin:** Supervision, Writing – review & editing, Resources, Project administration. **Pratheep Kumar Annamalai:** Conceptualization, Methodology, Supervision, Writing – review & editing.

Declaration of Competing Interest

The authors declare that they have no known competing financial interests or personal relationships that could have appeared to influence the work reported in this paper.

Data Availability

Data will be made available on request.

Acknowledgements

The authors thankfully acknowledge the Australian government for an international postgraduate research scholarship (IPRS), the University of Queensland living allowance scholarship and the University of Queensland continental scholarship. Pratheep Kumar Annamalai and Nasim Amiralian thank the Queensland Government for the Advance Queensland Research Fellowships. The authors acknowledge that this research utilizes Traditional Indigenous Knowledge which is owned and shared by Bulugudu Limited (formerly known as Dugalunji Aboriginal Corporation) on behalf of the Indjalandji-Dhidhanu peoples. Bulugudu Limited has also provided direct financial, equipment, and in-kind support to this project. The authors acknowledge Dr. Kenneth Tryggestad for proof reading and the staff in the Australian Microscopy and Microanalysis Research Facility at the Centre for Microscopy and Microanalysis (CMM, UQ), the University of Queensland.

Appendix A. Supporting information

Supplementary data associated with this article can be found in the online version at doi:10.1016/j.indcrop.2023.117729.

References

Abid, U., Gill, Y.Q., Irfan, M.S., Umer, R., Saeed, F., 2021. Potential applications of polycarbohydrates, lignin, proteins, polyacids, and other renewable materials for the formulation of green elastomers. Int. J. Biol. Macromol. 181, 1–29.

Annamalai, P.K., Dagnon, K.L., Monemian, S., Foster, E.J., Rowan, S.J., Weder, C., 2014. Water-responsive mechanically adaptive nanocomposites based on styrene-butadiene rubber and cellulose nanocrystals–processing matters. ACS Appl. Mater. Inter 6, 967–976.

Aziz, T., Ullah, A., Ali, A., Shabeer, M., Shah, M.N., Haq, F., Iqbal, M., Ullah, R., Khan, F. U., 2022. Manufactures of bio-degradable and bio-based polymers for bio-materials in the pharmaceutical field. J. Appl. Polym. Sci. 139, e52624.

Barana, D., Ali, S.D., Salanti, A., Orlandi, M., Castellani, L., Hanel, T., Zoia, L., 2016. Influence of lignin features on thermal stability and mechanical properties of natural rubber compounds. ACS Sustain. Chem. Eng. 4, 5258–5267.

Basti, A.T.K., Jonoobi, M., Sepahvand, S., Ashori, A., Siracusa, V., Rabie, D., Mekonnen, T.H., Naeijian, F., 2022. Employing cellulose nanofiber-based hydrogels for burn dressing. Polymers 14.

Bhattacharyya, S., Sinturel, C., Bahloul, O., Saboungi, M.L., Thomas, S., Salvetat, J.P., 2008. Improving reinforcement of natural rubber by networking of activated carbon nanotubes. Carbon 46, 1037–1045.

Bokobza, L., 2004. The reinforcement of elastomeric networks by fillers. Macromol. Mater. Eng. 289, 607–621.

Chang, B.P., Gupta, A., Muthuraj, R., Mekonnen, T.H., 2021. Bioresourced fillers for rubber composite sustainability: current development and future opportunities. Green. Chem. 23, 5337–5378.

Chen, J., Wu, J., Raffa, P., Picchioni, F., Koning, C.E., 2022. Superabsorbent polymers: from long-established, microplastics generating systems, to sustainable, biodegradable and future proof alternatives. Prog. Polym. Sci. 125, 101475.

Corletto, A., Hosseinmardi, A., Annamalai, P.K., Martin, D.J., Shapter, J.G., 2022. High-resolution R2R-compatible printing of carbon nanotube conductive patterns enabled by cellulose nanocrystals. ACS Appl. Nano Mater. 5, 1574–1587.

Diani, J., Fayolle, B., Gilormini, P., 2009. A review on the Mullins effect. Eur. Polym. J. 45, 601–612.

Ducrot, E., Creton, C., 2016. Characterizing large strain elasticity of brittle elastomeric networks by embedding them in a soft extensible matrix. Adv. Funct. Mater. 26, 2482–2492.

Ducrot, E., Chen, Y., Bulters, M., Sijbesma, R.P., Creton, C., 2014. Toughening elastomers with sacrificial bonds and watching them break. Science 344, 186–189.

Ducrot, E., Montes, H., Creton, C., 2015. Structure of tough multiple network elastomers by small angle neutron scattering. Macromolecules 48, 7945–7952.

Dwivedi, C., Manjare, S., Rajan, S.K., 2020. Recycling of waste tire by pyrolysis to recover carbon black: alternative & environment-friendly reinforcing filler for natural rubber compounds. Compos. Part B Eng. 200, 108346.

Fu, S.Y., Feng, X.Q., Lauke, B., Mai, Y.W., 2008. Effects of particle size, particle/matrix interface adhesion and particle loading on mechanical properties of particulate-polymer composites. Compos Part B-Eng. 39, 933–961.

Galant, O., Bae, S., Silberstein, M.N., Diesendruck, C.E., 2020. Highly stretchable polymers: mechanical properties improvement by balancing intra- and intermolecular interactions. Adv. Funct. Mater. 30.

Gao, B., Yang, J., Chen, Y., Zhang, S., 2021. Oxidized cellulose nanocrystal as sustainable crosslinker to fabricate carboxylated nitrile rubber composites with antibiosis, wearing and irradiation aging resistance. Compos. Part B Eng. 225, 109253.

Gil, A., 2021. Current insights into lignocellulose related waste valorization. Chem. Eng. J. Adv. 8, 100186.

Guimarães, B.M.R., Scatolino, M.V., Martins, M.A., Ferreira, S.R., Mendes, L.M., Lima, J. T., Junior, M.G., Tonoli, G.H.D., 2022. Bio-based films/nanopapers from lignocellulosic wastes for production of added-value micro-/nanomaterials. Environ. Sci. Pollut. Res. 29, 8665–8683.

Hosseinmardi, A., 2019. Reinforcement of natural rubber nanocomposites using lignocellulosic biomass, PhD Thesis, The University of Queensland, https://espace.library.uq.edu.au/view/UQ:d8b6d15.

Hosseinmardi, A., Annamalai, P.K., Wang, L., Martin, D., Amiralian, N., 2017. Reinforcement of natural rubber latex using lignocellulosic nanofibers isolated from spinifex grass. Nanoscale 9, 9510–9519.
Hosseinmardi, A., Annamalai, P.K., Martine, B., Pennells, J., Martin, D., Amiralian, N., 2018. Facile tuning of the surface energy of cellulose nanofibers for nanocomposite reinforcement. ACS Omega 3, 15933–15942.
Hosseinmardi, A., Amiralian, N., Hayati, A.N., Martin, D.J., Annamalai, P.K., 2021. Toughening of natural rubber nanocomposites by the incorporation of nanoscale lignin combined with an industrially relevant leaching process. Ind. Crops Prod. 159, 113063.
Ikeda, Y., Higashitani, N., Hijikata, K., Kokubo, Y., Morita, Y., Shibayama, M., Osaka, N., Suzuki, T., Endo, H., Kohjiya, S., 2009. Vulcanization: new focus on a traditional technology by small-angle neutron scattering. Macromolecules 42, 2741–2748.
Jagadeesh, P., Puttegowda, M., Rangappa, S.M., Siengchin, S., 2021. Influence of nanofillers on biodegradable composites: a comprehensive review. Polym. Compos. 42, 5691–5711.
Jiang, F., Li, T., Li, Y., Zhang, Y., Gong, A., Dai, J., Hitz, E., Luo, W., Hu, L., 2018. Wood-based nanotechnologies toward Sustainability. Adv. Mater. 30, 1703453.
John, M.J., Lefatle, M.C., Sithole, B., 2022. Lignin fractionation and conversion to bio-based functional products. Sustain. Chem. Pharm. 25, 100594.
Kazemi, H., Mighri, F., Park, K.W., Frikha, S., Rodrigue, D., 2022a. Natural rubber biocomposites reinforced with cellulose nanocrystals/lignin hybrid fillers. Polym. Compos. 43, 5442–5453.
Kazemi, H., Parot, M., Stevanovic, T., Mighri, F., Rodrigue, D., 2022b. Cellulose and lignin as carbon black replacement in natural rubber. J. Appl. Polym. Sci. 139.
Kumar, A.P., Singh, R.P., 2008. Biocomposites of cellulose reinforced starch: improvement of properties by photo-induced crosslinking. Bioresour. Technol. 99, 8803–8809.
Lay, M., Rusli, A., Abdullah, M.K., Abdul Hamid, Z.A., Shuib, R.K., 2020. Converting dead leaf biomass into activated carbon as a potential replacement for carbon black filler in rubber composites. Compos. Part B: Eng. 201, 108366.
Millereau, P., Ducrot, E., Clough, J.M., Wiseman, M.E., Brown, H.R., Sijbesma, R.P., Creton, C., 2018. Mechanics of elastomeric molecular composites. P Natl. Acad. Sci. USA 115, 9110–9115.
Mullins, L., 1969. Softening of rubber by deformation. Rubber Chem. Technol. 42, 339–362.
Nishimura, H., Kamiya, A., Nagata, T., Katahira, M., Watanabe, T., 2018. Direct evidence for alpha ether linkage between lignin and carbohydrates in wood cell walls. Sci. Rep. 8, 6538.
Olonisakin, K., fan, M., Xin-Xiang, Z., Ran, L., Lin, W., Zhang, W., Wenbin, Y., 2022. Key improvements in interfacial adhesion and dispersion of fibers/fillers in polymer matrix composites; focus on PLA matrix composites. Compos. Interfaces 29, 1071–1120.
Ozbas, B., Toki, S., Hsiao, B.S., Chu, B., Register, R.A., Aksay, I.A., Prud'homme, R.K., Adamson, D.H., 2012. Strain-induced crystallization and mechanical properties of functionalized graphene sheet-filled natural rubber. J. Polym. Sci. Pol. Phys. 50, 718–723.
Qiu, W., Zhang, F., Endo, T., Hirotsu, T., 2003. Preparation and characteristics of composites of high-crystalline cellulose with polypropylene: effects of maleated polypropylene and cellulose content. J. Appl. Polym. Sci. 87, 337–345.
Roy, K., Debnath, S.C., Pongwisuthiruchte, A., Potiyaraj, P., 2021. Recent advances of natural fibers based green rubber composites: properties, current status, and future perspectives. J. Appl. Polym. Sci. 138.
Sarkanen, S., Teller, D.C., Hall, J., Mccarthy, J.L., 1981. Lignin.18. associative effects among organosolv lignin components. Macromolecules 14, 426–434.
Sepahvand, S., Ashori, A., Jonoobi, M., 2023. Application of cellulose nanofiber as a promising air filter for adsorbing particulate matter and carbon dioxide. Int. J. Biol. Macromol. 244, 125344.
Setua, D.K., Shukla, M.K., Nigam, V., Singh, H., Mathur, G.N., 2000. Lignin reinforced rubber composites. Polym. Compos. 21, 988–995.
Sirviö, J.A., Hyypiö, K., Asaadi, S., Junka, K., Liimatainen, H., 2020. High-strength cellulose nanofibers produced via swelling pretreatment based on a choline chloride–imidazole deep eutectic solvent. Green. Chem. 22, 1763–1775.
Somaratne, M.C.W., Liyanage, N.M.V.K., Walpalage, S., 2014. Contribution of hydrogen and/or covalent bonds on reinforcement of natural rubber latex films with surface modified silica. J. Appl. Polym. Sci. 131.
Song, Y., Zheng, Q., 2016. A guide for hydrodynamic reinforcement effect in nanoparticle-filled polymers. Crit. Rev. Solid State Mater. Sci. 41, 318–346.
Tan, C., Peng, J., Lin, W., Xing, Y., Xu, K., Wu, J., Chen, M., 2015. Role of surface modification and mechanical orientation on property enhancement of cellulose nanocrystals/polymer nanocomposites. Eur. Polym. J. 62, 186–197.
Toki, S., Che, J., Rong, L.X., Hsiao, B.S., Amnuaypornsri, S., Nimpaiboon, A., Sakdapipanich, J., 2013. Entanglements and networks to strain-induced crystallization and stress-strain relations in natural rubber and synthetic polyisoprene at various temperatures. Macromolecules 46, 5238–5248.
Xue, C., Gao, H.Y., Hu, Y.C., Hu, G.X., 2019. Hyperelastic characteristics of graphene natural rubber composites and reinforcement and toughening mechanisms at multi-scale. Compos Struct. 228.
Yang, H.P., Yan, R., Chen, H.P., Lee, D.H., Zheng, C.G., 2007. Characteristics of hemicellulose, cellulose and lignin pyrolysis. Fuel 86, 1781–1788.
Yasin, S., Hussain, M., Zheng, Q., Song, Y., 2021. Effects of ionic liquid on cellulosic nanofiller filled natural rubber bionanocomposites. J. Colloid Interface Sci. 591, 409–417.
Zeng, H., Wasylczyk, P., Wiersma, D.S., Priimagi, A., 2018. Light robots: bridging the gap between microrobotics and photomechanics in soft materials. Adv. Mater. 30, e1703554.
Zhang, H.-C., Yu, C.-N., Li, X.-Z., Wang, L.-F., Huang, J., Tong, J., Lin, Y., Min, Y., Liang, Y., 2022. Recent developments of nanocellulose and its applications in polymeric composites. ES Food Agrofor. 9, 1–14.